A Cooperative SWIPT Scheme for Wirelessly Powered Sensor Networks

Tao Liu, Xiaodong Wang, *Fellow, IEEE*, and Le Zheng, *Member, IEEE*

***Abstract*— Wireless power transfer (WPT) provides a novel solution to the painstaking power-charging issue in wireless sensor networks. However, due to the propagation loss, the fast attenuation in energy transfer efficiency over the transmission distance is the main impediment to the WPT application. In this paper, we apply the simultaneous wireless information and power transfer (SWIPT) to a wirelessly powered sensor network, where each node has two circuits, which operate on energy harvesting mode and information decoding mode separately. We propose a novel cooperative SWIPT scheme (CSS) for this system. First, we present a conflict-free schedule initialization algorithm for CSS. For a given conflict-free schedule, we formulate a resource allocation problem to maximize the network energy efficiency, which is then transformed to an equivalent convex optimization problem and resolved via dual decomposition. Finally, a heuristic algorithm is presented to achieve the transmission schedule with the maximum energy efficiency and the corresponding resource assignment policy. Simulation results indicate that the CSS can significantly improve the energy efficiency of the wirelessly powered sensor network.**

***Index Terms*— Wireless sensor networks, wireless information and power transfer, energy efficiency, resource allocation.**

I. Introduction

WIRELESS sensor networks (WSNs) are made up of large quantities of sensor nodes with communication capabilities, and one or more sinks. In the WSN, the nodes collect data through the sensors and transmit them to the sinks via single hop or multi-hop communication. It is widely used in military and civil fields such as target tracking [1], intrusion detection [2] and surveillance applications [3].

Traditionally, sensor nodes use batteries as supply power. However, the energy scarcity of battery constitutes a major impediment to the applications of WSN. Thus, a considerable number of energy-aware protocols have been proposed to reduce energy consumption to increase the lifetime of a WSN. But these works are unable to provide a WSN with the ability to achieve uninterrupted long-term or perpetual operation. In order to resolve this problem, the EH technology has been applied to wireless sensor networks, where the EH device enables the sensor nodes to replenish the energy from ambient sources [5]–[9].

The conventional EH techniques enable the nodes to harvest energy from the natural sources, for instance, wind and solar, and store the harvested energy in the battery for future use if it can not be consumed immediately. But in general, the EH energy sources are stochastic in nature and therefore cannot reliably power a WSN uninterruptedly, even if the adaptive energy management and allocation scheme [5] is adopted. Due to this drawback of the conventional EH technique, new energy harvesting techniques like wireless power transfer (WPT) have emerged to power a WSN. Different from the conventional EH technique, WPT technique enables sensor nodes to charge their batteries from electromagnetic radiation, such as radio-frequency (RF) signals [11]. Compared with conventional EH techniques based on ambient energy sources, WPT is reliable and stable. Therefore, energy harvesting based on WPT is appropriate for low-power applications, such as sensor networks [12].

On the other hand, a major issue for WPT is the fast attenuation in energy transfer efficiency over the transmission distance because of the propagation loss. Hence this issue has great limits to the application of WPT. Therefore, a new method is needed to improve the energy transfer efficiency. Since RF signals that carry energy can at the same time be used as vehicle for transmitting information, a RF-based power transfer technology, named SWIPT [13] can be applied to improve the energy transfer efficiency. SWIPT can utilize both information and energy conveyed by RF signals simultaneously, whereas in traditional WSNs, the radio signal sent by a node can only be used by the destination node for information decoding. In this paper, we aim to maximize energy efficiency by taking advantage of SWIPT technique in wirelessly powered sensor networks. Specifically, our contributions are as follows:

- To resolve the energy transfer efficiency problem in a WPT-based WSN, we propose a novel Cooperative SWIPT Scheme (CSS). The superiority of CSS lies in integrating power charging with data transfer and efficiently utilizing the energy transported by the signals. Furthermore, this works aims at finding the conflict-free schedule and the optimal resource allocation policy so that the system energy efficiency is maximized.
- We propose a heuristic transmission schedule algorithm for CSS. This algorithm searches for a conflict-free schedule which can achieve maximum energy efficiency.

Manuscript received September 25, 2016; revised January 25, 2017 and March 12, 2017; accepted March 12, 2017. Date of publication March 22, 2017; date of current version June 14, 2017. This work was supported in part by the State Ethnic Science Research Project of China under grant 14XNZ030, the Key Project of Sichuan Provincial Department of Education under grant 15ZA0395, and the Leading Talents Program of Guangdong Province under grant 00201510. The associate editor coordinating the review of this paper and approving it for publication was D. Niyato. *(Corresponding author: Le Zheng.)*

T. Liu is with the School of Computer Science and Technology, Southwest Minzu University, Chengdu 610041, China (e-mail: swun_liu@hotmail.com).

X. Wang and L. Zheng are with the Electrical Engineering Department, Columbia University, New York, NY 10027 USA (e-mail: wangx@ee.columbia.edu; le.zheng.cn@gmail.com).

Color versions of one or more of the figures in this paper are available online at http://ieeexplore.ieee.org.

Digital Object Identifier 10.1109/TCOMM.2017.2685580

In particular, an initialization algorithm is proposed to establish the initial conflict-free schedule for the heuristic transmission schedule algorithm.

- For a given transmission conflict-free schedule, we formulate the cooperative power and information transfer problem in CSS as a non-convex optimization problem of finding the optimal resource allocation policy, which includes the transmission schedule, the transmission power allocation, the control of sensing data size and the energy broadcast time allocation to maximize the energy efficiency. This problem is transformed to an equivalent convex problem and then optimally resolved by the dual decomposition method.

The organization of the rest of this paper is as follows: Section II reviews related works. Section III depicts the system model and presents the CSS. Section IV presents a conflict-free schedule initialization algorithm. Section V formulates the resource assignment problem for a given transmission schedule and solves this problem. Section VI provides a heuristic algorithm to find a transmission schedule with high energy efficiency and the corresponding resource assignment. Section VII discusses the performance bound of CSS. Section VIII evaluates the system performance via simulations. Finally, the paper is summarized in Section IX.

II. Related Works

A. Ambient Energy Harvesting

To date, many works have used ambient energy harvesting techniques to power the wireless networks. Corke *et al.* [4] present the hardware design principles for long-term solar-powered wireless sensor networks. In [5], to maximize the network performance in the solar powered WSNs, the authors propose a distributed sampling rate control algorithm. Niyato *et al.* [6] present a queuing model to analyze the performances of different sleep and wakeup strategies in a solar-powered wireless sensor node. Other solar-powered sensor networks are illustrated in [7] and [8]. Meninger *et al.* [9] propose a system to convert ambient mechanical vibration into electrical energy for use in powering low power electronic systems. EU *et al.* [10] study different MAC protocols to coordinate the transmission of each WSN node powered by ambient energy harvesting.

However, the nature energy sources used in these works are time-varying and unreliable because of the time variations of harvested energy. Compared with other ambient energy harvesting techniques, the WPT technologies can provide the networks with stable energy supplies.

B. Wireless Power Transfer

Presently, there are two typical WPT technologies, which are respectively based on coupled magnetic resonances and RF signals. The former is explored by Kurs *et al.* [14] and WPT is realized by having magnetic resonant coils operate at the same resonance frequency so that they are strongly coupled via nonradiative magnetic resonance induction [15], [16]. However, energy transfer based on magnetic resonances is usually activated by near field induction from more powerful nodes (e.g., sink and vehicles).

Different from the coupled magnetic resonances, RF signal can convey both energy and information simultaneously. Thus, a RF-based energy harvesting technique, called SWIPT, realizes both useful utilizations of RF signals at the same time. Although this power transfer technique is still at the initial stage, there have been many researches on it in the literatures (e.g., [12], [17]–[21]). The core concept of SWIPT is that each node consists of two receiving circuits: EH circuit and information decoding (ID) circuit, which enable the nodes to harvest energy and decode information from the RF signals [13]. Based on these two circuits, in [12], two receiver designs, i.e., time switching and power splitting, are proposed. For time switching design (e.g., [19]–[21]), each node can switch between two modes, harvesting energy and decoding information mode, to either harvest energy or decode information, respectively; whereas for power splitting design (e.g., [17]), each node separates the received RF signal into two independent signal flows, one sent to the EH circuit and the other to the ID circuit. By dual utilization of RF signals for information and energy transfer, SWIPT enables wireless systems to achieve sustainable operation at a lower cost [12].

The works in [19]–[21] adopt the time-switching SWIPT technology. To control the tradeoff between information rate and harvested energy, a framework for scheduling multiple users in the downlink of a time-slotted SWIPT system with SWIPT is provided in [19]. In [20], a dynamic algorithm is presented to assign the time switching factor for minimizing the time average power consumption in the time-switching SWIPT systems. The joint transmit precoding and receiver time switching design for MISO SWIPT systems is also studied in [21]. However, these works consider the downlink transmission systems. Other works focus on the three-node networks [12] or one-hop networks [17], [18]. Hence these existing studies cannot be directly applied to the multihop WSN with multiple nodes.

C. Application of WPT in Wireless Sensor Networks

Recently, the WPT technology has been applied to power a WSN, for example, employing wireless chargers [22], [23], applying a mobile robot [16], [24]–[26], and replenishing energy from RF signals [27].

Tong *et al.* [22] use commercial RF-based WPT products [28], called Power-cast chips, to power up the batteries of sensor nodes in an experiment. This experiment validates the performance of the wireless charging technology for WSNs. Doost *et al.* [23] investigate the effect of distance and location on the energy transfer through electromagnetic waves. These works show that the WPT for a single node is inefficient. Therefore, WPT has some limitations when applied to a WSN because of low power transfer efficiency. Based on the WPT technology, a mobile robot or car is applied to carry a wireless charger to power a WSN in [16] and [24]–[26]. The robot or car periodically visits some predefined sensor positions to charge each sensor node. Though this technology significantly improves the power transfer efficiency, it leads

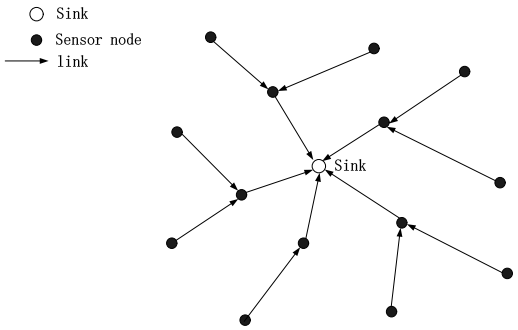

Fig. 1. The given data gathering tree of a sensor network.

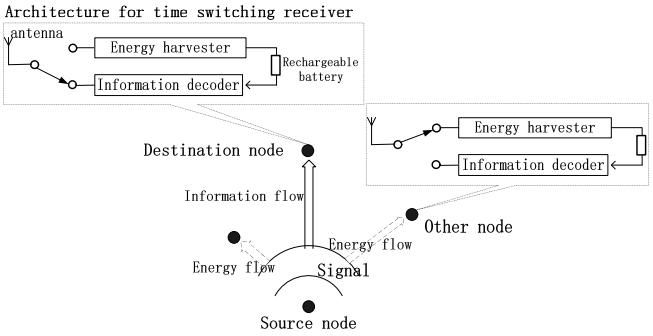

Fig. 2. SWIPT in the transmitting slot of a node.

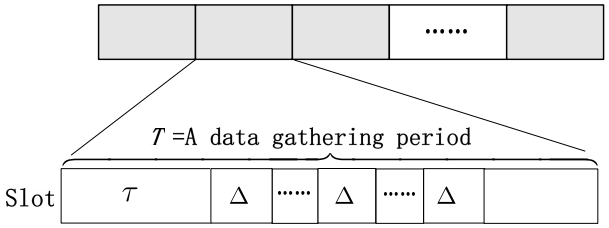

Fig. 3. Time slot assignment.

to much higher maintenance cost obviously or for some applications it is infeasible (e.g., for sensors embedded in building structures or inside human bodies).

In [12], RF signals are used to achieve SWIPT in a MIMO broadcasting system. However, this work studies the simple scenarios with only one or two user terminals. Tang *et al.* [29] consider a two-hop communication system. Assuming each relay can replenish energy from transmitted RF signals when the other relay transmits, they present an optimal transmission scheme. However, similar to [12], this scheme is only for the simplified networks with two-hop communication. In [30], SWIPT is applied to the clustered WSNs, where the nodes harvest RF signal. However, this paper focuses on the communication between two adjacent cluster heads instead of the sensor nodes and sink, whereas two adjacent cluster heads communicate directly or by one-hop relay. A further investigation is needed to study the multihop communication sensor network with a plurality of nodes.

D. Optimal Resource Allocation in Wireless Network

In the recent years, the study of optimal resource allocation in wireless networks has become an active research topic (e.g. [31]–[33]). In [31], to meet the QoS requirements of users in wireless networks, the utility-based resource allocation algorithms are presented. Tan *et al.* [32] develop the utility-based resource allocation algorithms in three different tasks and solve the network utility maximization problem. In [33], resource allocation for energy-efficient secure communication in OFDMA network is studied. Considering these researches are not targeted at the wirelessly powered sensor network, we should make a further study on finding the optimal resource allocation policy in the wirelessly powered sensor network.

III. System Descriptions

A. SWIPT-Powered Sensor Network for Data Collection

We consider a WSN which is composed of N sensor nodes and one sink. In this WSN, all sensor nodes are dispersed over the monitoring area and the sink is centrally located, as depicted in Fig. 1. The WSN is formulated as a directed graph $\mathcal{G} = (\mathcal{N}, \mathcal{L})$, where $\mathcal{N}$ denotes the set of vertices representing the sensor nodes, $N = |\mathcal{N}|$, $\mathcal{L} = \{l_{ij} | i, j \in \mathcal{N}\}$ and l_{ij} represents the wireless communication link from node i to j, which is denoted by the directed edge in Fig. 1. The links form a tree topology, which is referred to as a data gathering tree. Hence the data from each node is sent to the sink via a unique path on the tree. In fact, the data gathering tree is established based on the routing algorithms for WSNs (e.g., GBR [34]). Each node periodically sends its sensing data to the sink along the path on the data gathering tree. The sink not only receives the data from the nodes, but also broadcasts energy to all nodes. Thus, the whole network is powered by the sink.

Since both energy and information can be simultaneously carried by the RF signal, the same signal can be used to not only transmit information, but also charge the other nodes. As shown in Fig. 2, to enable SWIPT, each source node operates as both an information transmitter and an energy transferrer in its transmitting slot. The destination node works as an information receiver, while the other nodes work as energy harvesting receivers. Therefore, we adopt a practical "time switching" receiver design for a node, proposed in [12]. As depicted in Fig. 2, it is composed of a rechargeable battery and two circuits to operate on energy harvesting mode and information decoding mode separately. This design enables the node to adaptively operate on two work-modes, i.e., energy harvesting and information decoding modes.

B. Cooperative SWIPT Scheme

In order to improve energy transfer efficiency and avoid transmission collisions, we propose a cooperative SWIPT scheme (CSS), which is described bellow:

Time is divided into many data gathering periods, as shown in Fig. 3. Let T represent the duration of each data gathering period. To replenish energy and avoid collision, each data gathering period is divided into an energy broadcast slot and m data transmission slots. In the energy broadcast slot, the sink broadcasts RF signal, and all sensors harvest energy

and store the harvested energy in their batteries. The data transmission slots are equal in size and assigned to different sensor nodes. When some nodes transmit sensing data to the next-hop destination nodes in a slot, the destination nodes receive data and decode the information. Meanwhile, other nodes harvest wireless energy from the RF signal and store the harvested energy in their batteries. In other words, each node picks up a slot to transmit sensing data and harvests wireless energy in other time slots if they do not receive data. As illustrated in Fig. 3, τ denotes the duration of the energy broadcast slot and Δ denotes the duration of the data transmission slot. We assume $\tau + m\Delta \leq T$, where m is the total number of data transmission slots in a data gathering period.

Similar to prior work in [20], we assume the RF signals transmitted by the nodes are orthogonal to each other and do not interfere with each other. Therefore, it is possible to have multiple sensors to transmit data in the same data transmission slot as long as they do not conflict with each other.

On the other hand, to synchronize the clocks of the nodes, we adopt the reference broadcast synchronization (RBS) protocol [35] into the CSS. In some data gathering periods, the sink broadcasts a number of reference packets at the beginning of energy broadcast slot. Meanwhile, all nodes switch to information decoding mode, receive these packets and record their arrival time. Then the nodes exchange their recorded time stamps and estimate their relative phase offsets in the data transmission slots.

Based on the above scheme, our study focuses on finding the optimal policy, which includes the transmission schedule, the transmission power allocation, the control of sensing data size and the energy broadcast time allocation to maximize the energy efficiency.

IV. A Schedule Initialization Algorithm for CSS

In what follows, we present an algorithm to obtain a conflict-free and energy efficient initial schedule for CSS.

Similar to [36], a conflict graph can be used to model the conflict relation between wireless links. As shown in Fig. 4, the vertices of a conflict graph $\mathcal{F}$ correspond to the links in the connectivity graph $\mathcal{G}$. There is an edge between vertices l_{bd} and l_{ij} in $\mathcal{F}$ if the links l_{bd} and l_{ij} conflict with each other, that is, they have a node in common (i.e., $b = i$ or $d = i$ or $b = j$ or $d = j$). The conflict graph for a wireless network can be built in polynomial time [36]. For a given sensor network $\mathcal{G}$, we will find an initial conflict-free transmission schedule based on its conflict graph $\mathcal{F}$. Define a 0-1 variable α_{ij} such that $\alpha_{ij} = 1$ if node i cannot harvest wireless energy from node j when node j is transmitting data in a data transmission slot, which means node i is transmitting or receiving data in the same slot. Note that $\alpha_{ii} = 1$.

A simple upper bound on the number of data transmission slots in a conflict-free schedule is $m = N$. In this case, each slot is assigned to only one sensor node to transmit data, so the number of slots equals the number of sensor nodes in the network. Every node can harvest wireless energy from the maximum number of sensor nodes.

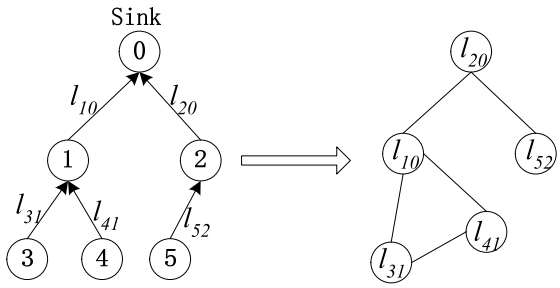

Fig. 4. Connectivity graph $\mathcal{G}$ and conflict graph $\mathcal{F}$.

Algorithm 1 Conflict-Free Schedule Initialization Algorithm

Inputs: Link set $\mathcal{L}$, conflict graph $\mathcal{F}$;
Outputs: maximal independent sets, initial schedule α_{ij};
1. $K = 1$;
2. Repeat
3. $\quad Q_K = \phi$;
4. $\quad$ Remove a link l_{ij} from $\mathcal{L}$; Add l_{ij} to Q_K;
5. $\quad$ For each link l_{pq} in $\mathcal{L}$
6. $\quad\quad$ If there is no edge between vertex l_{pq} and any vertex in Q_K according to $\mathcal{F}$
7. $\quad\quad$ Add link l_{pq} to Q_K; Remove l_{pq} from $\mathcal{L}$;
8. $\quad\quad$ End If
9. $\quad$ End For
10. $\quad K \leftarrow K + 1$;
11. Until $\mathcal{L} == \phi$
12. $\mathcal{S}_Q = \{Q_1, Q_2, \ldots, Q_K\}$;
13. For each Q_k in $\mathcal{S}_Q$
14. $\quad$ For any two links l_{ij} and l_{pq} in Q_k
15. $\quad\quad \alpha_{ji} = \alpha_{qp} = \alpha_{qi} = \alpha_{pi} = \alpha_{ip} = \alpha_{jp} = 1$;
16. $\quad$ End for
17. End for

On the other hand, to reduce the number of data transmission slots, we define the notion of maximal independent set. Given a conflict graph $\mathcal{F}$ with vertex set $\mathcal{L}$, an independent set is defined as a set of vertices such that there is no edge connecting arbitrary two vertices. A maximal independent set is the one that has the most vertices. Links in a independent set can be scheduled in the same slot. Let $Q_1, Q_2, \ldots, Q_K$, $(K \leq N)$ be a partition of the set $\mathcal{L}$, i.e., $\bigcup_{i=1}^{K} Q_i = \mathcal{L}$, $Q_i \cap Q_j = \phi$, $\forall i \neq j$, such that each Q_i is a maximal independent set.

Then we can assign a slot to each maximal independent set, so that the number of time slots equals the number of maximal independent sets (K). Thus, based on a conflict graph $\mathcal{F}$, we use Algorithm 1 below to obtain the partition of $\mathcal{L}$ into maximal independent sets and establish a conflict-free initial transmission schedule which has the least number of data transmission slots. In the next section, we formulate a resource assignment problem to maximize the energy efficiency of the wirelessly powered WSN for a given schedule.

V. Optimal Resource Allocation

A. Energy Consumption Model

Generally speaking, at each data gathering period, the energy consumption of a node can be divided into three parts, corresponding to the energy consumptions for data sensing/processing, data transmission and data reception, respectively. We define E_i^{con} as the energy consumption for node i in each data gathering period, which can be written as

$$E_i^{con} = r_i\varepsilon + \sum_{k\in I(i)} r_k e + p_i\Delta, \tag{1}$$

where r_i denotes amount of sensing data of node i in each data gathering period; ε and e denote the energy consumptions by a node for sensing/processing and receiving one unit data, respectively; p_i denotes the transmission power of node i, and $I(i)$ is the set of sensor nodes that use sensor node i as intermediate relay node (excluding sensor node i) on the data gathering tree, $i \in \mathcal{N}$. The first term represents the energy consumed by a node for data sensing/processing. The second term denotes the energy spent by data reception. The last term is the energy consumption for data transmission.

B. Energy Supply Model

According to the CSS, in each data gathering period, each sensor node harvests wireless energy from the sink in the energy broadcast slot and then harvests wireless energy when other nodes transmit data in their allocated slots. Note that a node cannot harvest wireless energy when it is transmitting or receiving data. Thus, the total amount of energy E_i harvested by node i in a data gathering period is

$$E_i = \eta h_{si} P_s \tau + \sum_{j=1}^{N} \eta h_{ji} p_j \Delta(1-\alpha_{ij}), \quad i \in \mathcal{N}, \tag{2}$$

where η denotes the energy conversion efficiency, $0 < \eta < 1$, P_s is the sink broadcasting power and h_{ij} denotes the channel power gain between node i and node j. Note that h_{si} denotes the channel power gain between the sink and node i. We have $h_{ij} = \kappa L_{ij}^{-\gamma}$ [30], where L_{ij} denotes the distance between nodes i and j, γ is a constant path loss exponent and κ is a normalization constant depending on the radio propagation properties of the environment. In (2), the first term denotes the amount of energy harvested from the sink and the second term represents the amount of energy harvested from the other nodes.

According to the energy-neutral operation [37], to ensure a sustainable network, the total amount of energy consumed by a node cannot be more than the amount of harvested energy in each data gathering period, namely,

$$E_i^{con} \le E_i, \quad \forall i \in \mathcal{N}. \tag{3}$$

Besides this, in order to keep the node sustainable in every slot, the occurrence of temporal death of each node must be avoided. The temporal death means the node depletes the energy of its battery and keeps the dead status until it harvests energy again [38]. In the kth data gathering period ($k \ge 1$), the residual energy stored in the battery of node i at the end of the bth slot ($1 \le b \le m$), denoted by $X_i(k,b)$, can be expressed as

$$\begin{aligned} X_i(k,b) = \Bigg(& x_i(0) + (k-1)(E_i - E_i^{con}) + \eta h_{si} P_s \tau \\ & + \sum_{j=1}^{N} \eta h_{ji} p_j \Delta\ (1-\alpha_{ij}) \cdot 1_{t_s(j)\le b} - r_i\varepsilon \cdot 1_{t_e(i)\le b} \\ & - p_i\Delta \cdot 1_{t_s(i)\le b} - \sum_{k\in I(i)} r_k e \cdot 1_{t_r(i)\le b} \Bigg)^+. \end{aligned} \tag{4}$$

where $(x)^+ = \max\{0, x\}$ and $x_i(0)$ denotes the total amount of initial energy stored in the battery of node i. The indicator function for an event A is represented by 1_A, it equals 1 if A occurs and is 0 otherwise. $t_s(i)$, $t_r(i)$ and $t_e(i)$ denote the transmitting, receiving and sensing slot number of node i, respectively. Note that $t_s(i)$ and $t_r(i)$ can be obtained from the transmission schedule. Particularly, the node goes into temporal dead status if $X_i(k,b) = 0$. Therefore, to avoid the occurrence of temporal death, in addition to condition (3), the condition $X_i(k,b) > 0$ should also be satisfied. Consequently, since $(k-1)(E_i - E_i^{con}) \ge 0$, $x_i(0)$ is lower bounded as follows

$$\begin{aligned} x_i(0) > {} & r_i\varepsilon \cdot 1_{t_e(i)\le b} + p_i\Delta \cdot 1_{t_s(i)\le b} \\ & + \sum_{k\in I(i)} r_k e \cdot 1_{t_r(i)\le b} - \eta h_{si} P_s \tau \\ & - \sum_{j=1}^{N} \eta h_{ji} p_j \Delta(1-\alpha_{ij}) \cdot 1_{t_s(j)\le b}. \end{aligned} \tag{5}$$

According to the optimized result, we can use (5) to obtain the lower bound of $x_i(0)$ for each node.

C. Channel Capacity Constraints

In each data gathering period, each node i senses and receives data, then transmits data in its allocated slot. We assume that the data buffer of each node has enough capacity to buffer all sensing data and received data. We assume that

$$r_i \ge r_{\min}, \quad \forall i \in \mathcal{N}, \tag{6}$$

where $r_{\min}$ denotes the minimum amount of sensing data limit for a node. Then the data rate of node i is given by

$$D_i = \frac{r_i + \sum_{k\in I(i)} r_k}{\Delta}. \tag{7}$$

According to the Shannon's formula, the channel capacity C_{id} between the node i and the node d with bandwidth ψ is

$$C_{id} = \psi \log_2\left(1 + \frac{p_i h_{id}}{\psi \sigma_{id}^2}\right), \tag{8}$$

where σ_{id}^2 denotes power spectral density of the additive white Gaussian noise (AWGN) in the channel between the source node i and the destination node d; h_{id} represents the channel power gain between the source node i and the destination node d; $\psi\sigma_{id}^2$ is the variance of AWGN at destination node d;

$\frac{p_i h_{id}}{\psi \sigma_{id}^2}$ is the signal-to-noise ratio (SNR) of the link. Therefore, the following channel capacity constraint must be satisfied

$$D_i \le C_{id}, \quad \forall i \in \mathcal{N}. \tag{9}$$

D. Optimization Problem

We define the network utility as

$$U = \sum_{i=1}^{N} \omega_i r_i, \tag{10}$$

where ω_i is a non-negative weight for node i. The energy consumption of sink in each data gathering period is given by

$$E = \tau P_s + \sum_{i=1}^{N} r_i e. \tag{11}$$

where e denotes the energy consumptions by a node for receiving one unit data. The first term indicates the total energy consumption of sink in the energy broadcasting slot. The second term is the energy consumption for receiving data from nodes. Since the whole network is powered by the sink, we define the network energy efficiency as the average utility received by sink per Joule consumed energy of sink, i.e.,

$$\xi = \frac{U}{E} = \frac{\sum_{i=1}^{N} \omega_i r_i}{\tau P_s + \sum_{i=1}^{N} r_i e}. \tag{12}$$

We aim to find the optimal resource allocation policy, which includes the transmission power allocation (p), the control of sensing data size (r) and the energy broadcast time allocation (τ), to maximize the energy efficiency ξ. That is, we have the following optimization problem

$$P1: \max_{\tau, p_i, r_i, i \in \mathcal{N}} \xi$$

Subject to

$$\begin{aligned}
&C1: E_i^{con} \le E_i, \quad i \in \mathcal{N} \\
&C2: D_i \le C_{id}, \quad \forall i \in \mathcal{N} \\
&C3: P_{\min} \le p_i \le P_{\max}, \quad i \in \mathcal{N} \\
&C4: r_i \ge r_{\min}, \quad i \in \mathcal{N} \\
&C5: \tau \le T - m\Delta, \\
&C6: \tau > 0, \quad C7: r_i > 0, \ C8: p_i > 0, \ i \in \mathcal{N}.
\end{aligned}$$

E. Alternative Formulation

Because of the fractional form of the objective function, problem $P1$ is nonconvex. In this subsection, we reformulate it as a convex problem. $P1$ is a convex-concave fractional problem [39], which is of the following form

$$\begin{aligned}
&\max \ \frac{f_0(\boldsymbol{x})}{\boldsymbol{c}^T x + d} \\
&\text{Subject to } \mathrm{f_i}\ (\boldsymbol{x}) \le 0, \quad \mathrm{i} = 1, \ldots, \mathrm{M} \\
&\qquad A\boldsymbol{x} = \boldsymbol{b},
\end{aligned}$$

where $\boldsymbol{x}$ is a vector of optimization variables, $\boldsymbol{c}$, $\boldsymbol{b}$ are constant vectors, d is a constant and A is a constant matrix. f_0 is concave, and $f_1 \ldots f_M$ are convex, and the domain of the objective function is $\{\boldsymbol{x} \in dom\ f_0 | \boldsymbol{c}^T \boldsymbol{x} + d > 0\}$. According to [39], by the following one-to-one variable transformation

$$\boldsymbol{y} = \frac{\boldsymbol{x}}{\boldsymbol{c}^T \boldsymbol{x} + d}, \quad z = \frac{1}{\boldsymbol{c}^T \boldsymbol{x} + d}$$

the problem above is equivalent to

$$\begin{aligned}
&\max \ g_0(\boldsymbol{y}, z) \\
&\text{Subject to } \mathrm{g_i}\ (\boldsymbol{y}, \mathrm{z}) \le 0, \quad \mathrm{i} = 1, \ldots, \mathrm{M} \\
&\qquad A\boldsymbol{y} = \boldsymbol{b}z \\
&\qquad \boldsymbol{c}^T \boldsymbol{y} + dz = 1,
\end{aligned}$$

where g_i is the perspective of f_i, namely

$$g_i(\boldsymbol{y}, z) = z f_i(\frac{\boldsymbol{y}}{z}), \quad i = 0, \ldots, M. \tag{13}$$

The above transformation shows that we can transform a convex-concave fractional problem into an equivalent convex optimization problem.

The numerator of the objective function of problem $P1$ is a linear function of variables r_i and hence it is both convex and concave. It can be easily proved that the constraints $C1 - C8$ of problem $P1$ are convex w.r.t. the optimization variables $\tau, r_i, p_i, \ i \in \mathcal{N}$. Besides, the denominator of the objective function of problem $P1$ is an affine function of τ and $r_i, \ i \in \mathcal{N}$. Thus, the above transformation can be applied. The variables z and $\boldsymbol{y} = \{y_{r_1} \ldots y_{r_N}, y_{p_1} \ldots y_{p_N}, y_\tau\}$ are introduced for variable transformation, where y_τ, y_{r_i}, y_{p_i} are the transformed variables of $\tau, r_i, p_i, \ i \in \mathcal{N}$ in the original problem, respectively. The relationship between the transformed variables and the original variables is

$$\tau = \frac{y_\tau}{z}, \quad r_i = \frac{y_{r_i}}{z}, \ p_i = \frac{y_{p_i}}{z}, \ i \in \mathcal{N}. \tag{14}$$

According to perspective operation [39], the equivalent problem $P2$ of problem $P1$ can be written as

$$\begin{aligned}
P2: \quad &\max_{z, y_\tau, y_{p_i}, y_{r_i}, i \in \mathcal{N}} \ \sum_{i=1}^{N} \omega_i y_{r_i} \\
&\text{Subject to } C1': y_{r_i}\varepsilon + \sum_{k \in I(i)} y_{r_k} e + y_{p_i}\Delta \le \eta h_{si} P_s y_\tau \\
&\qquad + \sum_{j=1}^{N} \eta h_{ji} y_{p_j} \Delta (1 - \alpha_{ij}), \quad \forall i \in \mathcal{N} \\
&\qquad C2': \frac{y_{r_i} + \sum_{k \in I(i)} y_{r_k}}{\Delta} \\
&\qquad\qquad \le z\psi \log_2\left(1 + \frac{y_{p_i} h_{id}}{z\psi\sigma_{id}^2}\right), \quad \forall i \in \mathcal{N} \\
&\qquad C3': z P_{\min} \le y_{p_i} \le z P_{\max}, \quad \forall i \in \mathcal{N} \\
&\qquad C4': \frac{z r_{\min}}{y_{r_i}} \le 1, \quad \forall i \in \mathcal{N} \\
&\qquad C5': y_\tau \le z(T - m\Delta), \\
&\qquad C6': y_\tau > 0, \quad C7': y_{r_i} > 0, \\
&\qquad C8': y_{p_i} > 0, \quad \forall i \in \mathcal{N}, \\
&\qquad C9': z > 0, \quad C10': P_s y_\tau + \sum_{i=1}^{N} e y_{r_i} = 1,
\end{aligned}$$

where constraints $C1' - C8'$ correspond to constraints $C1-C8$ of the problem $P1$, respectively. Note that $A = 0$. It is shown in [39] that perspective operation preserves concavity, i.e., if function f is convex, then so is its perspective function g. Similarly, if f is concave, then so is g. Since the numerator of the objective function of $P1$ is concave and the constraints $C1-C8$ of $P1$ is convex, we can prove the transformed optimization problem $P2$ is convex due to perspective operation. Because of the convexity of problem $P2$, the strong duality holds. Hence we can resolve the primal problem $P2$ by solving its dual problem, which will be discussed in the following subsection.

F. Dual Problem Formulation

Introducing multipliers to constraints $C1' - C5'$, the Lagrangian of problem $P2$ can be written as

$$\begin{aligned}
&L(z, y_\tau, y_p, y_r, \mu, \nu, \beta, \varphi, \theta, \lambda)\\
&= \sum_{i=1}^{N} \omega_i y_{r_i} + \sum_{i=1}^{N} \mu_i \left(\eta h_{si} P_s y_\tau + \sum_{j=1}^{N} \eta h_{ji} y_{p_j} \Delta \ (1-\alpha_{ij}) \right.\\
&\qquad \left. - y_{r_i}\varepsilon - \sum_{k\in I(i)} y_{r_k} e - y_{p_i}\Delta \right)\\
&\quad + \sum_{i=1}^{N} \nu_i \left(z\psi \log_2\left(1 + \frac{y_{p_i} h_{id}}{z\psi\sigma_{id}^2}\right) - \frac{y_{r_i} + \sum_{k\in I(i)} y_{r_k}}{\Delta} \right)\\
&\quad + \beta\left(z(T - m\Delta) - y_\tau\right) + \sum_{i=1}^{N} \varphi_i \left(y_{p_i} - z P_{\min}\right)\\
&\quad + \sum_{i=1}^{N} \theta_i \left(z P_{\max} - y_{p_i}\right) + \sum_{i=1}^{N} \lambda_i \left(1 - \frac{z r_{\min}}{y_{r_i}}\right). \qquad (15)
\end{aligned}$$

The constraints $C6' - C9'$ will be assimilated into the Karush-Kuhn-Tucker (KKT) conditions when deriving the solution later.

Rearranging the equality constraint $C10'$, we have

$$y_\tau = \frac{1 - \sum_{i=1}^{N} e y_{r_i}}{P_s}. \qquad (16)$$

Inserting (16) into (15), we can rewrite (15) as

$$\begin{aligned}
&L(z, y_\tau, y_p, y_r, \mu, \nu, \beta, \varphi, \theta, \lambda)\\
&= \sum_{i=1}^{N} \omega_i y_{r_i} + \sum_{i=1}^{N} \mu_i\\
&\quad \times \left(\eta h_{si} \left(1 - \sum_{i=1}^{N} e y_{r_i}\right) + \sum_{j=1}^{N} \eta h_{ji} y_{p_j} \Delta \ (1-\alpha_{ij}) \right.\\
&\qquad \left. - y_{r_i}\varepsilon - \sum_{k\in I(i)} y_{r_k} e - y_{p_i}\Delta \right)\\
&\quad + \sum_{i=1}^{N} \nu_i \left(z\psi \log_2\left(1 + \frac{y_{p_i} h_{id}}{z\psi\sigma_{id}^2}\right) - \frac{y_{r_i} + \sum_{k\in I(i)} y_{r_k}}{\Delta} \right)\\
&\quad + \beta \left(z(T - m\Delta) - \frac{1 - \sum_{i=1}^{N} e y_{r_i}}{P_s} \right) + \sum_{i=1}^{N} \varphi_i \left(y_{p_i} - z P_{\min}\right)\\
&\quad + \sum_{i=1}^{N} \theta_i \left(z P_{\max} - y_{p_i}\right) + \sum_{i=1}^{N} \lambda_i \left(1 - \frac{z r_{\min}}{y_{r_i}}\right). \qquad (17)
\end{aligned}$$

Thus, the dual function is given by

$$\begin{aligned}
&g(\mu, \nu, \beta, \varphi, \theta, \lambda)\\
&\qquad = \max_{z, y_\tau, y_p, y_r} L(z, y_\tau, y_p, y_r, \mu, \nu, \beta, \varphi, \theta, \lambda), \qquad (18)
\end{aligned}$$

subject to $C6' - C9'$. Then the dual problem of problem $P2$ is defined as

$$\min_{\mu,\nu,\beta,\varphi,\theta,\lambda} g(\mu, \nu, \beta, \varphi, \theta, \lambda). \qquad (19)$$

G. Optimal Solution to Dual Problem

We iteratively solve the dual problem (19) by decomposing it into two steps: 1) Step 1 computes the transformed optimization variables y_τ, y_p, y_r, z for given dual variables $\mu, \nu, \beta, \varphi, \theta, \lambda$; 2) Step 2 updates the dual variables $\mu, \nu, \beta, \varphi, \theta, \lambda$, based on the result of Step 1.

1) Step 1: First we solve the following primal problem

$$\begin{aligned}
&\max \ L(z, y_\tau, y_p, y_r, \mu, \nu, \beta, \varphi, \theta, \lambda)\\
&\text{Subject to C6}' - \text{C9}' \qquad (20)
\end{aligned}$$

for a fixed set of Lagrange multipliers $\mu, \nu, \beta, \varphi, \theta, \lambda$.

First, y_τ can be obtained by (16).

Then we can apply the Karush-Kuhn-Tucker (KKT) conditions [39] under nonnegative constraints. Since optimization variables z, y_p, y_r are positive, we have

$$\begin{aligned}
\frac{\partial L}{\partial y_{p_i}} &= -\mu_i \Delta + \nu_i z\psi \frac{h_{id}}{\ln 2 \times \ (z\psi\sigma_{id}^2 + y_{p_i} h_{id})}\\
&\quad + \varphi_i - \theta_i = 0, \quad i \in \mathcal{N}, \qquad (21)\\
\frac{\partial L}{\partial y_{r_i}} &= \omega_i - \sum_{k=1}^{N} e\mu_k \eta h_{sk} - \mu_i \varepsilon - \frac{\nu_i}{\Delta} + \frac{e\beta}{P_s}\\
&\quad + \frac{z\lambda_i r_{\min}}{y_{r_i}^2} = 0, \quad i \in \mathcal{N}, \qquad (22)\\
\frac{\partial L}{\partial z} &= \sum_{i=1}^{N} \nu_i \left(\psi \log_2\left(1 + \frac{y_{p_i} h_{id}}{z\psi\sigma_{id}^2}\right) - \frac{\psi y_{p_i} h_{id}}{\left(z\psi\sigma_{id}^2 + y_{p_i} h_{id}\right)\ln 2} \right)\\
&\quad + \beta(T - m\Delta) - \sum_{i=1}^{N} \varphi_i P_{\min} + \sum_{i=1}^{N} \theta_i P_{\max}\\
&\quad - \sum_{i=1}^{N} \frac{\lambda_i r_{\min}}{y_{r_i}} = 0. \qquad (23)
\end{aligned}$$

Rearranging (21) and (22), we obtain

$$y_{p_i} = z\left(\frac{\nu_i \psi}{(\mu_i \Delta - \varphi_i + \theta_i)\ln 2} - \frac{\sigma_{id}^2 \psi}{h_{id}} \right), \qquad (24)$$

$$y_{r_i} = \sqrt{\frac{z\lambda_i r_{\min}}{\sum_{k=1}^{N} e\mu_k \eta h_{sk} + \mu_i \varepsilon + \frac{\nu_i}{\Delta} - \frac{e\beta}{P_s} - \omega_i}}. \quad (25)$$

Inserting (24) and (25) into (23), we get

$$z = \left(\frac{\sum_{i=1}^{N} \sqrt{\left(\sum_{k=1}^{N} e\mu_k \eta h_{sk} + \mu_i \varepsilon + \frac{\nu_i}{\Delta} - \frac{e\beta}{P_s} - \omega_i \right) \lambda_i r_{\min}}}{Y} \right)^2, \quad (26)$$

where

$$Y = \sum_{i=1}^{N} \psi \nu_i \left(\log_2 \frac{h_{id}\nu_i}{(\mu_i \Delta - \varphi_i + \theta_i)\sigma_{id}^2 \ln 2} - \frac{1}{\ln 2} + \frac{\sigma_{id}^2 (\mu_i \Delta - \varphi_i + \theta_i)}{h_{id}\nu_i} \right) + \beta(T - m\Delta) - \sum_{i=1}^{N} \varphi_i P_{\min} + \sum_{i=1}^{N} \theta_i P_{\max}. \quad (27)$$

To sum up, for given $\mu, \nu, \beta, \varphi, \theta, \lambda$, we update z by (26) firstly. Then, according to the updated z, y_{p_i} and y_{r_i} are obtained by (24) and (25), respectively. Finally, based on the updated y_{r_i}, we use (16) to calculate y_τ.

2) Step 2: Next we utilize subgradient method to solve the dual problem defined in (19). Thus, the Lagrange multipliers updates are as follows

$$\mu_i(l+1) = \left[\mu_i(l) - \delta \left(\sum_{j=1}^{N} \eta h_{ji} y_{p_j}(l) \Delta (1 - \alpha_{ij}) + \eta h_{si} P_s y_\tau(l) - y_{r_i}(l)\varepsilon - \sum_{k \in I(i)} y_{r_k}(l) e - y_{p_i}(l) \Delta \right) \right]^+, \quad (28)$$

$$\nu_i(l+1) = \left[\nu_i(l) - \delta \left(z(l)\psi \log_2\left(1 + \frac{y_{p_i}(l) h_{id}}{z(l)\psi\sigma_{id}^2}\right) - \frac{y_{r_i}(l) + \sum_{k \in I(i)} y_{r_k}(l)}{\Delta} \right) \right]^+, \quad (29)$$

$$\beta(l+1) = [\beta(l) - \delta(z(l)(T - m\Delta) - y_\tau(l))]^+, \quad (30)$$

$$\varphi_i(l+1) = \left[\varphi_i(l) - \delta\left(y_{p_i}(l) - z(l) P_{\min}\right)\right]^+, \quad (31)$$

$$\theta_i(l+1) = \left[\theta_i(l) - \delta\left(z(l) P_{\max} - y_{p_i}(l)\right)\right]^+, \quad (32)$$

$$\lambda_i(l+1) = \left[\lambda_i(l) - \delta\left(1 - \frac{z(l) r_{\min}}{y_{r_i}(l)}\right) \right]^+, \quad (33)$$

where $i \in \mathcal{N}$ and l denotes the iteration index. δ represents a constant step size, $\delta > 0$ and $[\cdot]^+ = \max(\cdot, 0)$. Finally we summarize the optimal resource allocation algorithm for a given transmission schedule in Algorithm 2. Here, R^* is the optimal resource assignment policy of problem $P1$ for a given schedule, which includes the optimization variables z, τ, p_i and r_i, $i \in \mathcal{N}$. R_y is a transformed resource assignment policy of transformed problem $P2$, which includes the transformed variables z, y_τ, y_{p_i} and y_{r_i}, $i \in \mathcal{N}$. R_y^* denotes the optimal transformed resource assignment policy for a given schedule. By the one-to-one variable transformation using equations (14), we can obtain R^* from R_y^*. l_{max} denotes the maximum number of iterations. In each iteration of Algorithm 2, Step 2 updates Lagrange multipliers via the gradient update equations (28)-(33). Then Step 1 updates the transformed optimization variables based on the results of Step 2 and passes these updated variables to Step 2. This procedure is repeated until convergence is obtained or the maximum allowable number of iterations is reached.

Algorithm 2 Resource Allocation Algorithm

1. Initialization:
2. Initialize $\mu_i, \nu_i, \beta, \varphi_i, \theta_i, \lambda_i, y_\tau, z, y_{p_i}, y_{r_i}, i \in \mathcal{N}$;
3. $l = 0$, $R_y^* = \phi$, $R_y = \phi$;
4. Repeat
5. Update multipliers $\beta, \mu_i, \nu_i, \varphi_i, \theta_i, \lambda_i, i \in \mathcal{N}$ using (28)-(33);
6. According to updated multipliers, compute z by (26);
7. Compute $y_{p_i}, y_{r_i}, i \in \mathcal{N}$, using (24) and (25);
8. According to updated y_{r_i}, update y_τ by (16);
9. If $R_y == \{z, y_\tau, y_{p_i}, y_{r_i}, i \in \mathcal{N}\}$
10. $R_y^* = R_y$.
11. Else
12. $R_y = \{z, y_\tau, y_{p_i}, y_{r_i}, i \in \mathcal{N}\}$
13. End if
14. $l \leftarrow l + 1$;
15. If $l == l_{max}$
16. $R_y^* = R_y$
17. End if
18. Until $R_y^* \neq \phi$.
19. Transform R_y^* to R^* using (14).
20. Return R^*.

Theorem 1: For a constant step size δ, Algorithm 2 converges to R_y^*.

Proof: By using Equation (16),(24),(25) and (26), we can obtain a unique $R_y = \{z, y_\tau, y_{p_i}, y_{r_i}, i \in \mathcal{N}\}$. Since the Lagrangian multipliers $\beta, \mu_i, \nu_i, \varphi_i, \theta_i, \lambda_i$ can be obtain by optimization variables $z, y_\tau, y_{p_i}, y_{r_i}, i \in \mathcal{N}$ and network utility function is concave, there exists a step size δ which guarantees $\beta, \mu_i, \nu_i, \varphi_i, \theta_i, \lambda_i$ converge to the optimal dual solution $\zeta = \{\beta^*, \mu_i^*, \nu_i^*, \varphi_i^*, \theta_i^*, \lambda_i^*, i \in \mathcal{N}\}$ [40]. It is easy to find that $\nabla L(\zeta)$ satisfies Lipschitz continuous, because the curvatures of the utility function are bounded away from zero [41]. Therefore, Algorithm 2 with a constant step size δ, $0 < \delta < 2/\vartheta$, converges to the optimal transformed resource assignment policy R_y^*, where ϑ is the Lipschitz constant.

VI. Heuristic Transmission Scheduling Algorithm

Recall that in Section IV we started with an initial transmission schedule, for which we can compute the optimal resource allocation and the corresponding energy efficiency. Ideally we would like to find the transmission schedule with the maximum energy efficiency. However, enumerating all possible partitions of the data gathering tree in terms of independent sets is computationally prohibitive. Here we provide a heuristic algorithm to find a transmission schedule with high energy efficiency and the corresponding resource allocation policy. The proposed algorithm is given as Algorithm 3.

Algorithm 3 Heuristic Transmission Schedule Algorithm

Inputs: Link set $\mathcal{L}$, conflict graph $\mathcal{F}$;
Outputs: $\widetilde{\xi}$, $\widetilde{R}$, optimal schedule α_{ij};
1. Initialization:
   Use Algorithm 1 to obtain the maximal independent sets $Q_1, Q_2, \ldots, Q_K$ and establish the conflict-free initial schedule α_{ij};
   $\mathcal{S}_Q = \{Q_1, Q_2, \ldots, Q_K\}$;
   Set m to its lower bound, i.e., $m = K$; $\widetilde{\xi} = 0$.
2. Use Algorithm 2 to obtain intermediate optimal policies R^* and maximum energy efficiency ξ^* under this schedule;
3. If $\xi^* > \widetilde{\xi}$, $\widetilde{\xi} = \xi^*$, $\widetilde{R} = R^*$;
4. If $m = N$, then return $\widetilde{\xi}$, $\widetilde{R}$ and schedule α_{ij}, terminate the algorithm. Otherwise, go to step 5;
5. Pick the set Q, which has the most number of vertices, from the set $\mathcal{S}_Q$; Divide Q into two independent sets Q_1 and Q_2, Q_1 contains vertices $v_1, v_2, \ldots, v_{\lceil \frac{n}{2} \rceil}$ and Q_2 contains vertices $v_{\lceil \frac{n}{2} \rceil + 1}, \ldots, v_n$, n is the number of vertices in Q; Replace Q with Q_1, Q_2 in $\mathcal{S}_Q$;
   $m \leftarrow m + 1$;
6. Recompute schedule α_{ij};
7. Go to Step 2.

If a node transmits or receives data in slot k, it cannot harvest wireless energy from the nodes which are assigned slot k to transmit. Therefore, to increase the total amount of harvested energy of a node which transmits or receives data in slot k, we must decrease the number of links which are assigned slot k. Thus, in each iteration of Algorithm 3, we add a new slot to the schedule and perform a new slot assignment. To achieve the greatest increase of harvested energy of nodes, Algorithm 3 finds the slot which is assigned to most number of links and breaks these links into two sets which are assigned to two slots.

The framework of Algorithm 3 is given by Fig. 5 and we summarize Algorithm 3 as follows. Algorithm 3 starts with the maximal independent sets and initial transmission schedule α_{ij} obtained by using algorithm 1. Then we use an iterative process to look for higher energy efficiency. In each iteration, for a given transmission schedule α_{ij}, we use Algorithm 2 to obtain intermediate optimal policies R^* and maximum energy efficiency ξ^* under this schedule. In Algorithm 2, we firstly establish optimization problem $P1$ which aims to maximize the energy efficiency. Then we transform problem $P1$ into an equivalent convex optimization problem $P2$. Finally, we resolve the problem $P2$ by solving its dual problem (19). After that, we adjust the schedule α_{ij} by performing a new slot assignment. This procedure is repeated until the number of time slots reaches the upper bound, which equals the number of sensor nodes in the network.

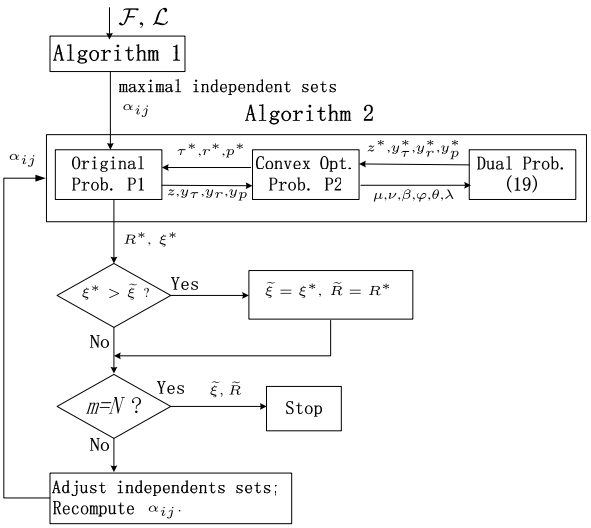

Fig. 5. The framework of Algorithm 3.

We now analyze the time complexity of Algorithm 3. It consists of two loops. The outer loop is to search for a transmission schedule which can achieve maximum energy efficiency. The number of iteration of outer loop can be given by $N-K+1$. On the other hand, the inner loop is to update the optimization variables and Lagrange multipliers. In the worst case, the number of iterations of inner loop is l_{max}. Hence the time complexity of Algorithm 3 is $O(l_{\max} \times (N-K+1))$.

VII. Performance Bound Analysis

In this section, we derive the performance bound of CSS. To do this, we investigate the maximum cooperative energy transfer ratio of each node. The cooperative energy transfer ratio of a node is defined as the ratio of the energy harvested from other nodes to the energy directly harvested from the sink in each data gathering period. For better cooperative energy transfer ratio, a node should harvest most energy from other nodes via cooperative energy transfer in each data gathering period. The following theorem states the upper bound for the harvested energy from other nodes in each data gathering period.

Theorem 2: B_i denotes the total amount of harvested energy from other nodes for node i in each data gathering period, which is upper bounded as follows

$$B_i \leq \sum_{k=1}^{\infty} \chi_k, \tag{34}$$

where χ_k $(k \geq 1)$ are given by

$$\chi_1 = \sum_{j_1=1}^{N} \left[\eta h_{j_1\ i}(1-\alpha_{ij_1})(\eta h_{sj_1} P_s \tau)\right],$$

$$\chi_k = \sum_{j_1=1}^{N} \cdots \sum_{j_k=1}^{N} \left[\eta^k h_{j_1\ i}(\prod_{b=2}^{k} h_{j_b j_{b-1}})(1-\alpha_{ij_1}) \times (\prod_{b=2}^{k}(1-\alpha_{j_{b-1}j_b}))(\eta h_{sj_k} P_s \tau)\right], \quad k \geq 2.$$

Proof: Note that each node switches its operations periodically between harvesting energy and broadcasting wireless energy. Hence, each node can be viewed as power-transfer relay, which relays energy between a node or sink and other nodes via wireless power transfer. In order to ensure that the node can harvest most of the energy, the other nodes only work as energy relays. Therefore, the maximum amount of harvesting energy from other nodes for node i can be divided into several parts depending on the number of hops of relay.

For the two-hop relay, node j_1 $(j_1 \in \mathcal{N})$ relays energy between the sink s and node i. Thus, the first part is computed by

$$\chi_1 = \sum_{j_1=1}^{N} \left[\eta h_{j_1 i}(1-\alpha_{ij_1})(\eta h_{sj_1} P_s \tau)\right] \tag{35}$$

Furthermore, the kth part is the energy harvested from other nodes via $k+1$ hop relay and follows

$$\chi_k = \sum_{j_1=1}^{N} \cdots \sum_{j_k=1}^{N} \left[\eta^k h_{j_1 i}(\prod_{b=2}^{k} h_{j_b j_{b-1}})(1-\alpha_{ij_1}) \times (\prod_{b=2}^{k}(1-\alpha_{j_{b-1}j_b}))(\eta h_{sj_k} P_s \tau)\right]. \tag{36}$$

where $k \geq 2$. The nodes $j_1, j_2, \ldots, j_k$ relay energy via $k+1$ hop between the sink s and node i. Note that the k hop energy relay transfer is completed within k data gathering periods. The maximum harvested energy for node i in each data gathering period can be obtained by summing up χ_k for $k = 1, 2, \ldots, \infty$. This completes the proof of Theorem 2.

According to Theorem 2, the maximum cooperative energy transfer ratio of node i is given by

$$\zeta_i^m = \frac{\sum_{k=1}^{\infty} \chi_k}{\eta h_{si} P_s \tau} \tag{37}$$

where $\eta h_{si} P_s \tau$ is the total amount of energy harvested directly from the sink in the energy broadcast slot. We then expand the size of the network and investigate the change of the maximum cooperative energy transfer ratio of a node. Suppose the distance between every two nodes is increased by n times, i.e., $\widetilde{L_{ij}} = nL_{ij}$ $(n > 1)$, where $\widetilde{L}$ is the distance after expansion. The maximum cooperative energy transfer ratio of a node is

$$\widetilde{\zeta_i^m} = \frac{\sum_{k=1}^{\infty} \widetilde{\chi_k}}{\widetilde{\eta h_{si}} P_s \tau} \tag{38}$$

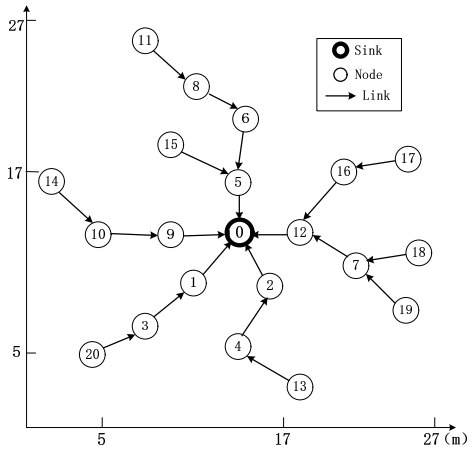

Fig. 6. Network topology.

Since $h_{ij} = \kappa L_{ij}^{-\gamma}$, $\widetilde{h_{ij}} = \kappa n^{-\gamma} L_{ij}^{-\gamma} = n^{-\gamma} h_{ij}$, we have

$$\widetilde{\zeta_i^m} = \frac{\sum_{k=1}^{\infty} n^{-k\gamma} \chi_k}{\eta h_{si} P_s \tau} \tag{39}$$

Since $0 < \eta < 1$, η^k is very small when k is large enough. Thus, it is easy to obtain the approximate value of $\widetilde{\zeta_i^m}$. According to the formula (39), the maximum cooperative energy transfer ratio of a node decreases with the growth of n. To evaluate the performance bound of CSS, we introduce a threshold of the averaged maximum cooperative energy transfer ratio for all nodes. If the average maximum cooperative energy transfer ratio for all nodes is less than this threshold, the energy harvested from other nodes is too small in comparison with the energy directly harvested from the sink. On this basis, we can compute the maximum size of the network by finding a parameter n that enables average maximum cooperative energy transfer ratio to equal the given threshold.

VIII. Simulation Results

In this section, the simulation results are provided to show the performance of CSS for the network scenario shown in Fig. 6. Specifically, we consider a WSN with 20 sensor nodes, 1 sink node, and 20 links. Unless otherwise stated, we set the parameters as follows: $\Delta = 1s, T = 20s$, $N = 20, P_{max} = 1 \times 10^{-2} W, P_{min} = 1 \times 10^{-9} W, P_s = 0.1W, \eta = 0.8, \varepsilon = 200\ nJ, e = 50nJ, r_{min} = 1 \times 10^3, \kappa = 1, \gamma = 2, \psi = 1 \times 10^3 Hz$. We assume all nodes have the same weight $\omega_i = 1 (i \in \mathcal{N})$ and all channels have the same variance of AWGN, i.e., $\psi \sigma_{id}^2 = 5 \times 10^{-7} W (i \in \mathcal{N}, (i,d) \in \mathcal{L})$. We compare CSS with three other WPT schemes, including the non-cooperative WPT scheme, non-optimal schedule WPT scheme and WPT scheme with fixed transmission power. Similar to CSS, these WPT schemes divide each data gathering period into an energy broadcast slot and several data transmission slots and assign data transmission slots to sensor nodes for transmitting and receiving data. The sink broadcasts energy in the energy broadcast slot. Unlike

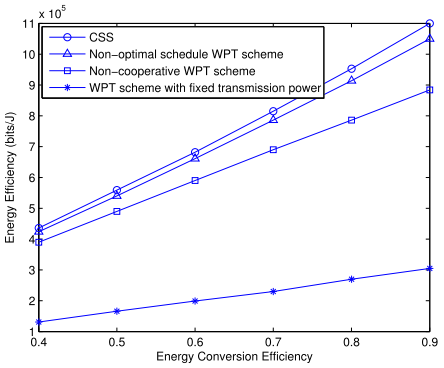

Fig. 7. Energy efficiency vs. energy conversion efficiency.

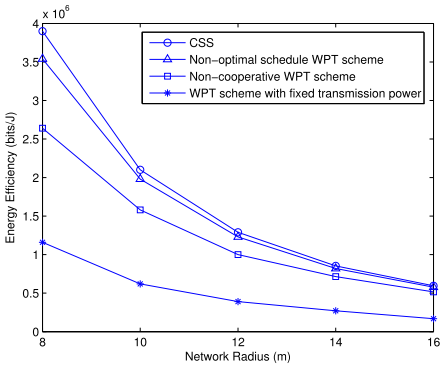

Fig. 9. Energy efficiency vs. network radius.

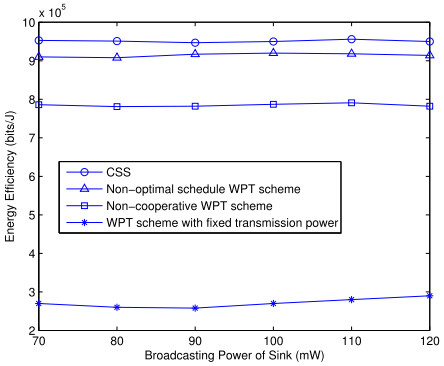

Fig. 8. Energy efficiency vs. sink broadcasting power.

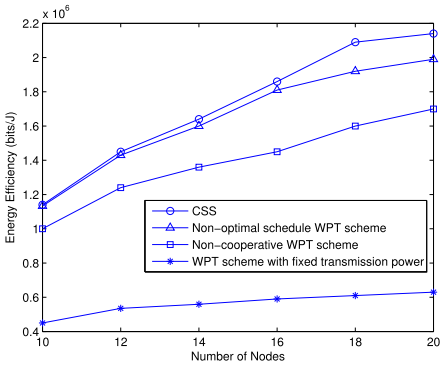

Fig. 10. Energy efficiency vs. number of nodes.

CSS, in the non-cooperative WPT scheme, all nodes harvest wireless energy only in the energy broadcast slot when the sink broadcasts wireless energy. In the non-optimal schedule WPT scheme, instead of looking for the suboptimal schedule, the transmission schedule is according to the initial schedule computed by Algorithm 1. As for WPT scheme with fixed transmission power, all nodes transmit data with the same fixed power and we let the transmission power equal to $2 \times 10^{-4} W$.

Firstly, we evaluate the impact of energy conversion efficiency (η) on energy efficiency for different schemes. Fig. 7 depicts the relationship between the energy efficiency and the energy conversion efficiency.

We observe from Fig. 7 that the energy efficiency in all schemes increases with the increase of energy conversion efficiency. This is because higher energy conversion efficiency leads to more harvested energy from RF signals. Another observation is that CSS exhibits higher energy efficiency of network over other schemes. This is because each node harvests wireless energy from other nodes in addition to the sink in CSS. Therefore, compared to non-cooperative WPT scheme, CSS increases the amount of energy harvested by each node, which leads to more data sensed by each node. Moreover, the optimal schedule and optimal transmission power allocation in CSS can improve the energy efficiency of network.

Next, we investigate the impact of broadcasting power of sink on energy efficiency. Fig. 8 depicts the energy efficiency of network versus the broadcasting power of sink for the four schemes. As shown in Fig. 8, the CSS performs better than other schemes. Moreover, we can find that the energy efficiency of network under different broadcasting power of sink for four schemes is nearly equal. This is because the nodes harvest more energy and generate more sensing data in each data gathering period when the broadcasting power of the sink increases. It means the network utility increases with the increase of the broadcasting power of sink. As a result, the energy efficiency of network under different broadcasting power of sink is nearly equal.

Then we consider a circular field, where the radius varies during the experiments. The sink is centrally located in this circular field and 20 sensor nodes are uniformly distributed in the circular field. It can be seen in Fig. 9 that when the network radius increases, the energy efficiency decreases for all schemes. This is because since all nodes are uniformly distributed in the circular field, the average distance between two nodes increases when the radius increases, which leads to lower channel power gains. As a result, the average total amount of harvested energy for a node in each data gathering period decreases with the increase of the radius. On the other hand, we can observe that CSS achieves the highest energy efficiency.

Fig. 10 indicates the relationship between the energy efficiency and the total number of nodes. Note that all sensor nodes are uniformly distributed in a circular field and the radius of the circular field is 10m. We can see from Fig. 10 for all four schemes, the energy efficiency increases with the increase of the number of nodes. This is because that the total

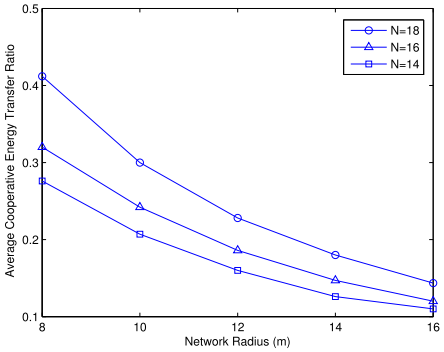

Fig. 11. Average cooperative energy transfer ratio vs. network radius.

amount of data sensed will increase, as the number of nodes increases. Moreover, the CSS performs better than other three schemes.

To evaluate the performance of CSS, we investigate the impact of network radius on average cooperative energy transfer ratio for all nodes. As shown in Fig. 11, in the CSS, the average cooperative energy transfer ratio decreases when network radius increases. This is because the amount of energy harvested from other nodes decreases quickly with the increase of the network radius. Another observation is that a higher average cooperative energy transfer ratio is achieved while the total number of nodes increases. This is because CSS makes a sensor node harvest more energy from other nodes if more sensor nodes are deployed in the network.

IX. Conclusions

This paper has proposed applying the SWIPT technology to wirelessly powered sensor networks. We aim to find optimal policies, which includes transmission schedule, transmission power allocation, the control of sensing data size and the energy broadcast time allocation to maximize energy efficiency and ensure the perpetual operation of wirelessly powered sensor networks. To achieve this goal, we have proposed a novel Cooperative SWIPT Scheme that consists of a conflict-free schedule initialization algorithm, a cooperative resource allocation algorithm and a heuristic algorithm to obtain the transmission schedule with maximum energy efficiency and the corresponding resource allocation policy. Simulation results show that the CSS can maximize energy efficiency of the wirelessly powered sensor network.

References

[1] H. T. Kung and D. Vlah, "Efficient location tracking using sensor networks," in *Proc. IEEE Wireless Commun. Netw. Conf.*, vol. 3. Mar. 2003, pp. 1954–1961.

[2] Y. Wang, X. Wang, B. Xie, D. Wang, and D. P. Agrawal, "Intrusion detection in homogeneous and heterogeneous wireless sensor networks," *IEEE Trans. Mobile Comput.*, vol. 7, no. 6, pp. 698–711, Jun. 2008.

[3] T.-L. Chin and W.-C. Chuang, "Latency of collaborative target detection for surveillance sensor networks," *IEEE Trans. Parallel Distrib. Syst.*, vol. 26, no. 2, pp. 467–477, Feb. 2015.

[4] P. Corke, P. Valencia, P. Sikka, T. Wark, and L. Overs, "Long-duration solar-powered wireless sensor networks," in *Proc. EmNets*, Cork, Ireland, Jun. 2007, pp. 33–37.

[5] Y. Zhang, S. He, J. Chen, Y. Sun, and X. S. Shen, "Distributed sampling rate control for rechargeable sensor nodes with limited battery capacity," *IEEE Trans. Wireless Commun.*, vol. 12, no. 6, pp. 3096–3106, Jun. 2013.

[6] D. Niyato, E. Hossain, and A. Fallahi, "Sleep and wakeup strategies in solar-powered wireless sensor/mesh networks: Performance analysis and optimization," *IEEE Trans. Mobile Comput.*, vol. 6, no. 2, pp. 221–236, Feb. 2007.

[7] K. Lin *et al.*, "Heliomote: Enabling long-lived sensor networks through solar energy harvesting," in *Proc. Sensys*, San Diego, CA, USA, Nov. 2005, p. 309.

[8] S. Yang, X. Yang, J. A. McCann, T. Zhang, G. Liu, and Z. Liu, "Distributed networking in autonomic solar powered wireless sensor networks," *IEEE J. Sel. Areas Commun.*, vol. 31, no. 12, pp. 750–761, Dec. 2013.

[9] S. Meninger, J. O. Mur-Miranda, R. Amirtharajah, A. Chandrakasan, and J. H. Lang, "Vibration-to-electric energy conversion," *IEEE Trans. Very Large Scale Integr. (VLSI) Syst.*, vol. 9, no. 1, pp. 64–76, Feb. 2001.

[10] Z. A. Eu, H.-P. Tan, and W. K. G. Seah, "Design and performance analysis of MAC schemes for wireless sensor networks powered by ambient energy harvesting," *Ad Hoc Netw.*, vol. 9, no. 3, pp. 300–323, May 2011.

[11] M. Y. Naderi, P. Nintanavongsa, and K. R. Chowdhury, "RF-MAC: A medium access control protocol for re-chargeable sensor networks powered by wireless energy harvesting," *IEEE Trans. Wireless Commun.*, vol. 13, no. 7, pp. 3926–3937, Jul. 2014.

[12] R. Zhang and C. K. Ho, "MIMO broadcasting for simultaneous wireless information and power transfer," *IEEE Trans. Wireless Commun.*, vol. 12, no. 5, pp. 1989–2001, May 2013.

[13] X. Zhou, R. Zhang, and C. K. Ho, "Wireless information and power transfer: Architecture design and rate-energy tradeoff," *IEEE Trans. Commun.*, vol. 61, no. 11, pp. 4754–4767, Nov. 2013.

[14] A. Kurs, A. Karalis, R. Moffatt, J. D. Joannopoulos, P. Fisher, and M. Soljačić, "Wireless power transfer via strongly coupled magnetic resonances," *Science*, vol. 317, no. 5834, pp. 83–86, Jul. 2007.

[15] M. Zhao, J. Li, and Y. Yang, "A framework of joint mobile energy replenishment and data gathering in wireless rechargeable sensor networks," *IEEE Trans. Mobile Comput.*, vol. 13, no. 12, pp. 2689–2705, Dec. 2014.

[16] S. Guo, C. Wang, and Y. Yang, "Joint mobile data gathering and energy provisioning in wireless rechargeable sensor networks," *IEEE Trans. Mobile Comput.*, vol. 13, no. 12, pp. 2836–2852, Dec. 2014.

[17] H. Chen, Y. Li, Y. Jiang, Y. Ma, and B. Vucetic, "Distributed power splitting for SWIPT in relay interference channels using game theory," *IEEE Trans. Wireless Commun.*, vol. 14, no. 1, pp. 410–420, Jan. 2015.

[18] E. Boshkovska, D. W. K. Ng, N. Zlatanov, and R. Schober, "Practical non-linear energy harvesting model and resource allocation for SWIPT systems," *IEEE Commun. Lett.*, vol. 19, no. 12, pp. 2082–2085, Dec. 2015.

[19] R. Morsi, D. S. Michalopoulos, and R. Schober, "Multiuser scheduling schemes for simultaneous wireless information and power transfer over fading channels," *IEEE Trans. Wireless Commun.*, vol. 14, no. 4, pp. 1967–1982, Apr. 2015.

[20] Y. Dong, M. J. Hossain, and J. Cheng, "Joint power control and time switching for SWIPT systems with heterogeneous QoS requirements," *IEEE Commun. Lett.*, vol. 20, no. 2, pp. 328–331, Feb. 2016.

[21] N. Janatian, I. Stupia, and L. Vandendorpe, "Joint multi-objective transmit precoding and receiver time switching design for MISO SWIPT systems," in *Proc. IEEE SPAWC*, Edinburgh, Scotland, Jul. 2016, pp. 1–5.

[22] B. Tong, Z. Li, G. Wang, and W. Zhang, "How wireless power charging technology affects sensor network deployment and routing," in *Proc. IEEE ICDCS*, Genoa, Italy, Jun. 2010, pp. 438–447.

[23] R. Doost, K. R. Chowdhury, and M. Di Felice, "Routing and link layer protocol design for sensor networks with wireless energy transfer," in *Proc. IEEE GLOBECOM*, Miami, FL, USA, Dec. 2010, pp. 1–5.

[24] Y. Peng, Z. Li, W. Zhang, and D. Qiao, "Prolonging sensor network lifetime through wireless charging," in *Proc. IEEE RTSS*, San Diego, CA, USA, Nov./Dec. 2010, pp. 129–139.

[25] L. Xie, Y. Shi, Y. T. Hou, and H. D. Sherali, "Making sensor networks immortal: An energy-renewal approach with wireless power transfer," *IEEE/ACM Trans. Netw.*, vol. 20, no. 6, pp. 1748–1761, Dec. 2012.

[26] L. He, L. Kong, Y. Gu, J. Pan, and T. Zhu, "Evaluating the on-demand mobile charging in wireless sensor networks," *IEEE Trans. Mobile Comput.*, vol. 14, no. 9, pp. 1861–1875, Sep. 2015.

[27] T. Ajmal, D. Jazani, and B. Allen, "Design of a compact RF energy harvester for wireless sensor networks," in *Proc. IET Wireless Sensor Syst.*, London, U.K., Jun. 2012, pp. 1–5.
[28] PowerCast Corp. [Online]. Available: http://www.powercastco.com
[29] L. Tang, X. Zhang, and X. Wang, "Joint data and energy transmission in a two-hop network with multiple relays," *IEEE Commun. Lett.*, vol. 18, no. 11, pp. 2015–2018, Nov. 2014.
[30] S. Guo, F. Wang, Y. Yang, and B. Xiao, "Energy-efficient cooperative transmission for simultaneous wireless information and power transfer in clustered wireless sensor networks," *IEEE Trans. Commun.*, vol. 63, no. 11, pp. 4405–4417, Nov. 2015.
[31] L. Tan and Y. Zhang, "Optimal resource allocation with principle of equality and diminishing marginal utility in wireless networks," *Wireless Pers. Commun.*, vol. 84, no. 1, pp. 671–693, Sep. 2015.
[32] L. Tan, Z. Zhu, F. Ge, and N. Xiong, "Utility maximization resource allocation in wireless networks: Methods and algorithms," *IEEE Trans. Syst., Man, Cybern., Syst.*, vol. 45, no. 7, pp. 1018–1034, Jul. 2015.
[33] D. W. K. Ng, E. S. Lo, and R. Schober, "Energy-efficient resource allocation for secure OFDMA systems," *IEEE Trans. Veh. Technol.*, vol. 61, no. 6, pp. 2572–2585, Jul. 2012.
[34] C. Schurgers and M. B. Srivastava, "Energy efficient routing in wireless sensor networks," in *Proc. IEEE Military Commun. Conf. (MILCOM)*, vol. 1. McVean, VA, USA, Oct. 2001, pp. 357–361.
[35] J. Elson, L. Girod, and D. Estrin, "Fine-grained network time synchronization using reference broadcasts," in *Proc. 5th Symp. Oper. Syst. Design Implement.*, Boston, MA, USA, Dec. 2002, pp. 147–163.
[36] M. Cheng, Q. Ye, and L. Cai, "Cross-layer schemes for reducing delay in multihop wireless networks," *IEEE Trans. Wireless Commun.*, vol. 12, no. 2, pp. 928–937, Feb. 2013.
[37] A. Kansal, J. Hsu, S. Zahedi, and M. B. Srivastava, "Power management in energy harvesting sensor networks," *ACM Trans. Embedded Comput. Syst.*, vol. 6, no. 4, pp. 32–38, Sep. 2007.
[38] L. Tan and S. Tang, "Energy harvesting wireless sensor node with temporal death: Novel models and analyses," *IEEE/ACM Trans. Netw.*, vol. 1, pp. 168–177, 2006, doi: 10.1109/TNET.2016.2607229.
[39] S. Boyd and L. Vandenbergh, *Convex Optimization*. Cambridge, U.K.: Cambridge Univ. Press, 2004.
[40] D. P. Bertsekas, *Nonlinear Programming*, 2nd ed. Belmont, MA, USA: Athena Scientific, 1999.
[41] S. H. Low and D. E. Lapsley, "Optimization flow control. I. Basic algorithm and convergence," *IEEE/ACM Trans. Netw.*, vol. 7, no. 6, pp. 861–874, Dec. 1999.

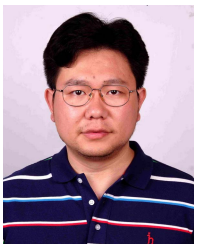

Tao Liu received the B.S. degree from the Nanjing University of Posts and Telecommunications, the M.S. degree from the University of Electronic Science and Technology of China, and the Ph.D. degree from Sichuan University, China, all in computer science. He was a Visiting Scholar with Columbia University, New York, NY, USA, from 2015 to 2016. He is currently an Associate Professor with the School of Computer Science and Technology, Southwest Minzu University, Chengdu, China. His current research interests include ad hoc networks and wireless sensor networks.

Xiaodong Wang (S'98–M'98–SM'04–F'08) received the Ph.D. degree in electrical engineering from Princeton University. He is currently a Professor of Electrical Engineering with Columbia University, New York, NY, USA. His current research interests include wireless communications, statistical signal processing, and genomic signal processing. He has served as an Associate Editor of the IEEE TRANSACTIONS ON COMMUNICATIONS, the IEEE TRANSACTIONS ON WIRELESS COMMUNICATIONS, the IEEE TRANSACTIONS ON SIGNAL PROCESSING, and the IEEE TRANSACTIONS ON INFORMATION THEORY. He is listed as an ISI Highly-cited Author.

Le Zheng received the B.S. degree in communication engineering from Northwestern Polytechnical University, Xi'an, China, in 2009, and the Ph.D. degree in target detection and recognition from the Beijing Institute of Technology, Beijing, China, in 2015. From 2013 to 2014, he was a Visiting Scholar with the Electrical Engineering Department, Columbia University, New York, NY, USA, where he is currently a Post-Doctoral Researcher. His research interests include statistical signal processing, radar system, and wireless sensor networks.